Accelerated Publications

Quantitative and Real-Time Detection of Secretion of Chemical Messengers from Individual Platelets[†]

Shencheng Ge, Nathan J. Wittenberg, and Christy L. Haynes*

Department of Chemistry, University of Minnesota, Minneapolis, Minnesota 55455

Received March 13, 2008; Revised Manuscript Received June 3, 2008

ABSTRACT: Carbon-fiber microelectrochemical methods were utilized in this study to measure individual exocytotic events of secretion of serotonin and histamine from washed rabbit platelets. The quantal release of serotonin was quantitatively characterized with a δ-granule serotonin concentration of 0.6 M and secretion time course of 7 ms. Additionally, extracellular osmolarity influences quantal size, causing quantal size increases under hypotonic conditions, presumably due to the influx of cytosolic serotonin into the halo region of the δ-granules.

Normal platelet function is essential to hemostasis. Upon activation, platelets secrete a variety of clotting factors, small signaling molecules, and the neurotransmitter serotonin. Platelets are the major storage cells for serotonin in the circulatory system (*1*). They take up free serotonin and package it into dense-body granules (δ-granules) along with adenine nucleotides, inorganic ions, and pyro- and polyphosphate. Platelets share many biochemical adaptations for serotonergic activity with neurons of the central nervous system, such as the presence of serotonin transporters, serotonin receptors, and vesicular monoamine transporters, and thus provide an interesting, but different, system in which to study neurotransmitter dynamics (*2*). Assays for serotonin content and secretion from platelets typically rely on established technologies, such as radiometric assays (*3*) and chromatographic separations (*4*). These assays, while time-tested and reliable, have poor temporal resolution for measuring secreted serotonin and give results in the form of ensemble averages from millions of cells. Ensemble averages mask the properties of individual cells and make discovery of cellular subpopulations impossible. In this paper, we demonstrate the ability to detect and chemically identify individual serotonin secretion events from isolated, single rabbit platelets. We employ fast-scan cyclic voltammetry (FSCV) and amperometry, electroanalytical methods with submillisecond temporal resolution that have been applied to the study of exocytosis for nearly two decades (*5*). From our amperometric studies, we were able to determine the number of δ-granules released per platelet, evaluate the time course of release of serotonin from individual δ-granules, calculate the number of serotonin molecules contained in each δ-granule, and, in combination with previously published TEM data, determine the concentration of serotonin in δ-granules. Furthermore, the amperometric study allows us to make inferences about the time course of secretion from δ-granules for other electroinactive messengers in the clotting cascade, such as ADP, ATP, and calcium. In addition, we evaluate the effects of altered extracellular osmolarity on exocytosis. Our voltammetric studies demonstrated the corelease of serotonin and histamine from single granules in rabbit platelets, a phenomenon highly analogous to that in cultured mast cells from mouse and rat first demonstrated by the Wightman research group using the same method (*6*–*8*). Using these high-resolution electrochemical methods, we are able to determine the temporal and chemical features of normal platelet secretion. This will allow us to move forward in examining chemical messenger uptake, storage, and release from platelets altered either by pharmacology, particularly antidepressants, or by disease, such as Hermansky-Pudlak syndrome, a platelet storage pool disorder (*9*).

Washed rabbit platelets were prepared according to previously published procedures (*10*). Carbon-fiber microelectrodes for amperometry and FSCV experiments (Figure 1A) were fabricated according to published procedures (*11*) with minor modifications (see the Supporting Information). Platelets were activated with a 3 s pressure ejection of 10 μM ionomycin from a glass micropipette located adjacent to the cell. All data herein are reported as means $\pm$ the standard error of the mean. For all of the statistical comparisons, unpaired Student's *t* tests were performed.

δ-Granules have been long recognized as a storage pool for serotonin in a variety of animal species (*12*). Here, FSCV was employed to chemically identify the stored amines. Among the well-characterized contents of the δ-granules, only serotonin and histamine can be measured at the applied potentials using a bare carbon-fiber microelectrode; detection

[†] This study is supported by the Kinship Foundation Searle Scholar Program.

* To whom correspondence should be addressed: Department of Chemistry, University of Minnesota, 207 Pleasant St. SE, Minneapolis, MN 55455. E-mail: chaynes@umn.edu. Telephone: (612) 626-1096. Fax: (612) 626-7541.

10.1021/bi800792m CCC: $40.75
Published on Web 06/17/2008

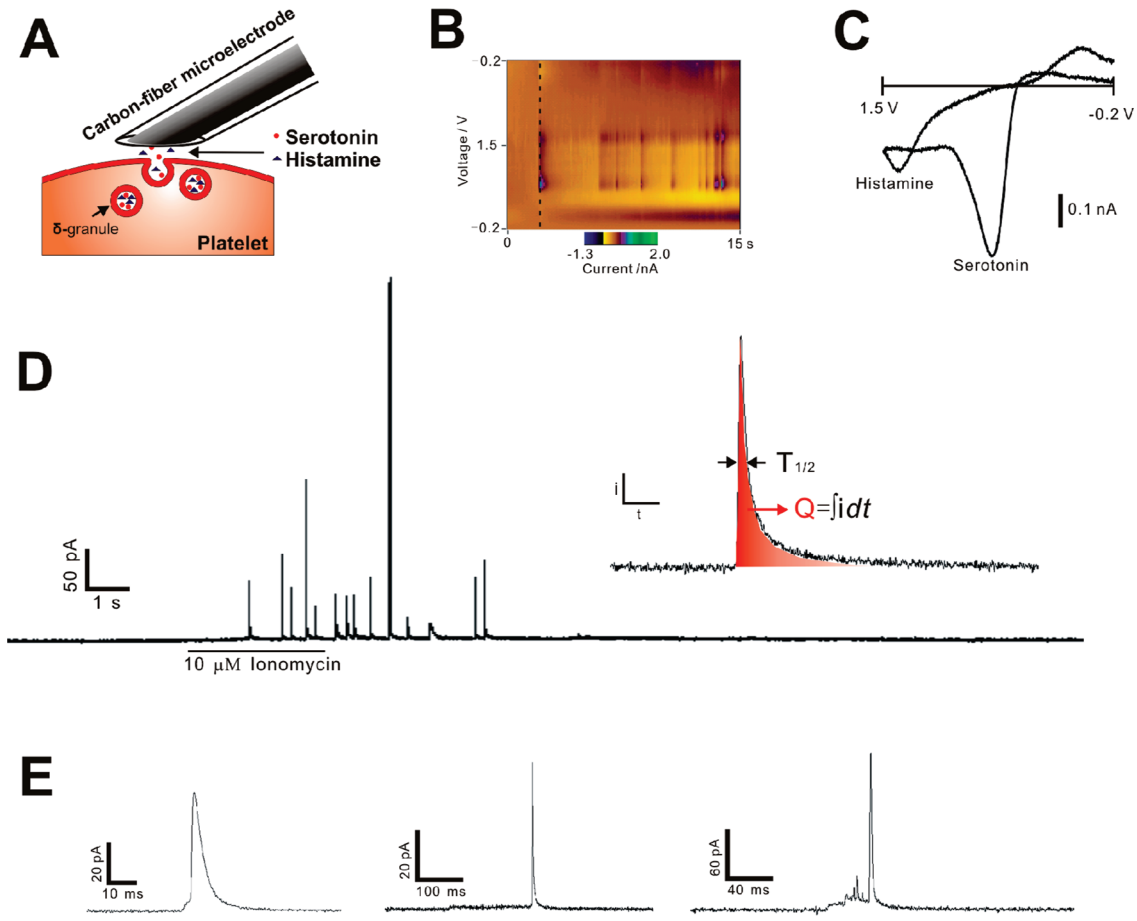

FIGURE 1: Electrochemical measurements on single platelets. (A) Schematic depicting a typical experimental setup with a carbon-fiber microelectrode placed close to the platelet plasma membrane. The δ-granules within the activated platelet fuse with the plasma membrane and release their contents; the electroactive components are immediately sensed by the carbon-fiber microelectrode. The size of the platelet shown is not drawn to scale to show the granular fusion events. (B) When a fast triangular voltage ramp from −0.2 to 1.5 V and back to −0.2 V at a rate of 400 V/s is repetitively applied to the carbon-fiber electrode every 100 ms, the resulting currents from capacitive charging (charging current) and oxidation or reduction of the released molecules (faradaic current) are recorded during each waveform application. After subtraction of the stable charging current, only the amplitude of the faradaic current is encoded by false color and presented herein. Each blue-green spot at approximately 0.7 V (*y*-axis) represents the oxidation of serotonin released from individual δ-granules, while the less pronounced blue-green spot at approximately 1.4 V (*y*-axis) indicates the oxidation of histamine. The concurrence of oxidation events for serotonin and histamine reveals that these two molecules are stored and released from the same granules. (C) A representative fast-scan cyclic voltammogram of serotonin and histamine is extracted from the false color plot by replotting the faradaic current against the applied voltage during a voltage ramp, which is shown by the dotted line on the false color plot. (D) When the carbon-fiber microelectrode is held at 0.7 V (vs a Ag/AgCl reference electrode), only serotonin, not histamine, released from a δ-granule is sensed by the carbon-fiber microelectrode as a current transient which can be characterized by spike area and half-width (full width at half-maximum, $t_{1/2}$) which are shown in the inset. The platelet is activated by elevating the intracellular calcium concentration by injecting 10 μM ionomycin onto the cell for 3 s, represented by the black bar below the trace. (E) A minority of the recorded current spikes display a prespike foot feature which indicates the formation and maintenance of a nanoscale fusion pore ahead of full fusion between the granular membrane and the cell plasma membrane. A spike with a typical foot is shown at the left. Rarely, extra long and fluctuating prespike feet may occur and are shown in the center and at the right, respectively.

of other redox-active species such as ADP, ATP, and adenine requires either significantly larger potential excursions or alternate electrode materials (*13, 14*). FSCV on bare carbon-fiber microelectrodes has also been successfully applied by others in identifying a variety of electroactive molecules during exocytosis, including dopamine (*15*), serotonin (*6*), and histamine (*6*). Using FSCV, panels B and C of Figure 1 show direct evidence of release of serotonin from δ-granules in platelets based on the location of the oxidation and reduction peaks (*6*). Interestingly, the coincidence of oxidation peaks for histamine and serotonin in the FSCV color plot reveals that rabbit platelets costore and corelease histamine from the same δ-granules. This costorage of histamine and serotonin in the same granule was previously postulated by Da Prada et al. in ensemble-averaged measurements from rabbit platelets (*16*). While our data confirm conclusions drawn from previous ensemble experiments, our techniques will allow us to identify cellular and granular subpopulations, such as cells or granules that secrete either serotonin or histamine, but not both molecules. Identification of subpopulations is not possible with ensemble measurements because they are simply averages of millions of cells assayed simultaneously. Addressing individual cells in this fashion will provide interesting insights into chemical messenger storage and release from platelets from a variety of mammalian species and have far-reaching impacts in vascular biology.

Until now, it has been technically challenging to accurately extract quantitative data about secretion from individual platelet δ-granules. Exploiting the aforementioned electro-

chemical methods, we are able to measure the quantal size, the amount of chemical messenger secreted from an individual granule, of δ-granule serotonin with unprecedented accuracy. In rabbit platelets, amperometry data (Figure 1D) yield a mean spike area or charge, Q, of 205 ± 17 fC under isotonic conditions (averaged 1134 spikes from 39 platelets), which is equivalent, using Faraday's law, to (6.4 ± 0.5) × 10^5 serotonin molecules secreted from each δ-granule (*17*). The potential applied to the working electrode for amperometry (+0.7 V vs Ag/AgCl) lies above the half-wave potential for serotonin, but below that of histamine, ensuring that only serotonin molecules are detected. Using an estimated rabbit δ-granule diameter of 150 nm (*18*), the granular concentration of serotonin is calculated to be 0.6 M. The same synergistic combination of electrochemical and electron microscopy data can be applied to calculate the quantal size of serotonin in human platelets or platelets from any other animal species. Using this approach to determine the quantal size, granular concentration, and number of granules secreted, diseases of platelet storage pool dysfunction, such as Hermansky-Pudlak syndrome, where both the number of δ-granules and serotonin storage efficiency are decreased, could be identified and potential therapeutics evaluated. In addition, the role of platelets in regulation of hyperserotonemia (elevated plasma serotonin concentration) (*19*) could be investigated in great detail.

Beyond gaining quantitative information about granular storage and release using amperometry, we can also gain unique insights into how platelets subtly modulate serotonin release upon close examination of spike appearance. Specifically, a prespike feature, known as a foot (Figure 1E), indicates an intermediate stage of granule−plasma membrane fusion when serotonin is released through a narrow pore spanning the granular and cytoplasmic membrane (*20, 21*). In the amperometric traces recorded from individual platelets, the appearance, and thus the release behavior, of the foot feature is highly heterogeneous. For example, foot duration varies from ∼5 ms (first panel in Figure 1E) to ∼200 ms (second panel in Figure 1E). In addition, the amplitude of the foot signal can change significantly during long periods of fusion pore maintenance. In contrast to the foot behavior in the first two panels of Figure 1E, the foot shown in the third panel displays dynamic current fluctuation before the full fusion spike. The difference in chemical messenger delivery through the fusion pore indicates a relatively stable docking state between two membranes in the first two examples and a flickering fusion pore before full fusion in the third example. Similar results were recently observed by Lindau and co-workers during exocytosis of catecholamine from bovine chromaffin cells as measured using the patch-amperometry method (*20*). In this work, they demonstrated that the narrow fusion pore acts as a diffusion barrier for granular catecholamine molecules to escape during exocytosis. Herein, it is possible to quantitatively characterize this semistable fusion pore in platelets, offering a unique opportunity to probe a variety of physiologically relevant factors affecting this cell communication modality. Future work will explore how cholesterol and ethyl alcohol, known to alter lipid bilayer fluidity, change the ability of platelets to maintain this semistable release pathway.

The osmolarity of blood in the circulatory system is tightly regulated; however, previous studies by Pollard and co-workers demonstrated that the bulk efficiency of release of serotonin from human platelets could be altered by extracellular osmotic pressure (*22*). Because carbon-fiber microelectrode amperometry facilitates observation of single release events, it is possible to quantitatively clarify the underlying mechanistic change with varied extracellular conditions. In this study, we alter the osmolarity of the experimental medium to determine the effects of both hyper- and hypotonicity on the characteristics of individual serotonin exocytosis events. Determination of how altered ionic conditions perturb normal serotonin storage and secretion by platelets could shed light on the mechanism by which hyponatremia (depressed plasma sodium level, sometimes, accompanied by decreased plasma osmolarity) is a side effect of selective serotonin reuptake inhibitor (SSRI) treatment for clinical depression (*23*). Systematic studies also give insight into the fundamental driving forces behind delivery of chemical messengers from δ-granules. Herein, it is revealed that the average number of released δ-granules per rabbit platelet does not significantly change ($p > 0.01$) with varied osmotic conditions, which is shown in Figure 2B; however, the mean spike area, 313 ± 29 fC, under hypotonic conditions is significantly larger ($p < 0.001$, one-tailed) than that under isotonic conditions, 205 ± 17 fC. This increased spike area indicates that the δ-granules secrete an average of 3.4 × 10^5 more serotonin molecules, that is, have a larger quantal size, under low-extracellular osmotic pressure conditions. Thus, the change in quantal size, rather than the number of granules successfully fusing, is responsible for the increased release efficiency observed under hypotonic conditions. In prior work, increased quantal size under hypotonic conditions was observed in amperometric studies in bovine adrenal chromaffin cells by Schroeder and co-workers (*24*). We further hypothesize that these newly incorporated serotonin molecules under hypotonic conditions can be attributed to the influx of serotonin from cytosol into δ-granules as the original serotonin balance is disturbed by cellular and granular bloating. The granular swelling is strongly supported by examining the distribution of $Q^{1/3}$, which reflects the radius distribution of δ-granules (*25*). As shown in Figure 2A, the $Q^{1/3}$ distribution under hypotonic conditions is significantly broader than that under isotonic conditions, clearly indicating the volume change in δ-granules. For a detailed discussion of how granular volume expansion results in a broadened $Q^{1/3}$ distribution, see the Supporting Information. The observed volume change is likely the result of increased "halo" volume between dense body and granular membrane, a region that acts as a storage pool for newly imported cytosolic serotonin. Neither the quantal size nor the $Q^{1/3}$ distribution varies significantly between isotonic and hypertonic conditions. Together, these data indicate that the halo volume is stable and smaller under these two conditions. In future work, the variation of halo volume will be further explored with electron microscopy studies.

Amperometry studies also facilitate exploration of the effects of osmolarity on the kinetics of chemical messenger secretion by considering the spike half-width [$t_{1/2}$ (Figure 1D)]; this characteristic reveals the time required for expansion or dissolution of the δ-granule core to liberate chemical messengers. Additionally, analysis of the occurrence of the prespike foot features (Figure 1E) gives insights into the balance between granular membrane tension and the driving

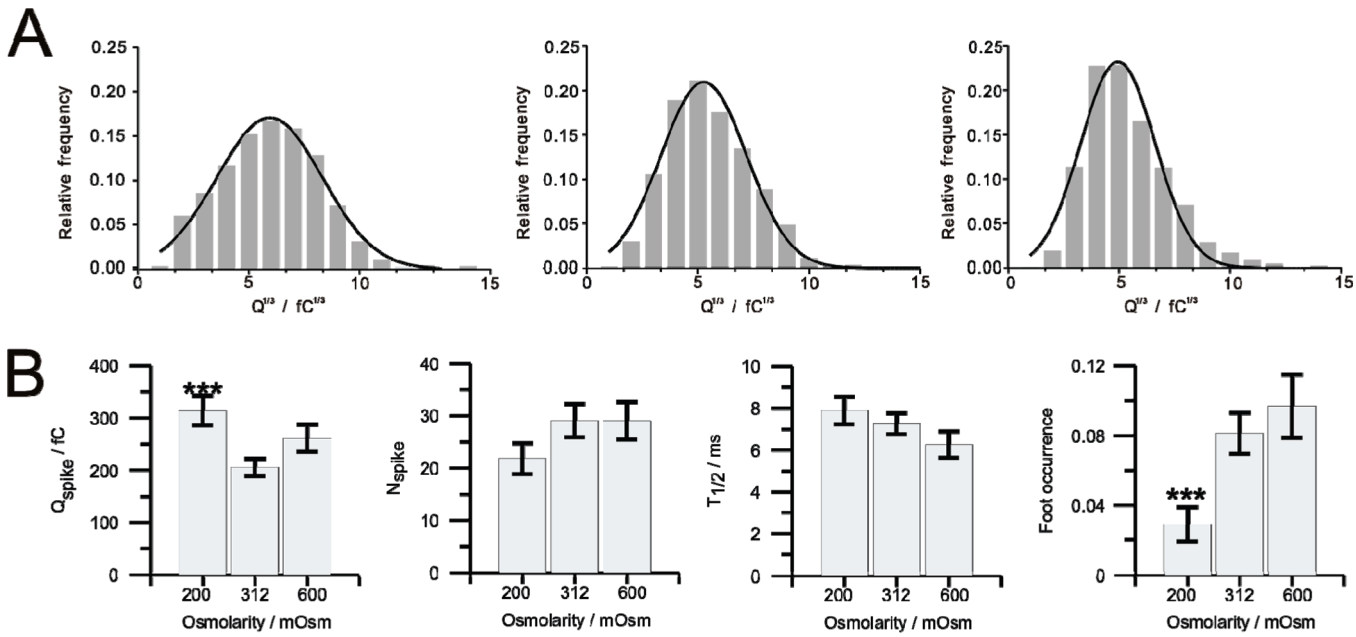

FIGURE 2: Statistical analysis of spike parameters from serotonin exocytosis recorded using amperometry. (A) Three distribution charts of the cubic root of spike area, $Q^{1/3}$, constructed individually from all the amperometric spikes under each condition (approximately 1000 spikes recorded from approximately 40 individual platelets in each case). This $Q^{1/3}$ distribution is a reflection of the radius distribution of δ-granules from a large pool of single platelets because each value of Q is proportional to individual granular volume, that is, $(4\pi/3) - r^3$, if all δ-granules in a given cell share the same concentration. Each $Q^{1/3}$ histogram is best fit by a Gaussian distribution which is shown as a black line. The standard deviations for the fits are 2.37, 1.93, and 1.67 $fC^{1/3}$ for hypotonic, isotonic, and hypertonic conditions, respectively. (B) Spike area, number of spikes per platelet, spike full width at half-maximum ($t_{1/2}$), and prespike foot occurrence are statistically compared under hypotonic, isotonic, and hypertonic conditions using unpaired Student's t tests where the values under isotonic conditions are used as controls. This analysis reveals that spike area is significantly larger ($p < 0.001$, one-tailed), while the prespike foot occurrence per platelet is significantly lower ($p < 0.001$) under hypotonic conditions compared to those under isotonic and hypertonic conditions. However, no statistical difference is observed ($p > 0.01$) for either the number of spikes per platelet or $t_{1/2}$ under any osmotic condition.

forces for granular content release. In this work, no statistical difference in $t_{1/2}$ is observed among the varied osmolarity conditions, even with the aforementioned changes in quantal size. This kinetic consistency regardless of extracellular osmolarity is sensible on the basis of our current knowledge of dense-body composition and the fact that the dissociation of nonprotein constituents (such as serotonin, ATP, and ADP) from the dense body should be independent of extracellular osmolarity for physiological purposes. This characteristic of platelets is in stark contrast to trends measured in chromaffin (*26*), mast (*27*), and PC-12 cells (*28*) where high extracellular osmolarity suppresses the unfolding of proteinaceous dense-core material, leading to a larger measured $t_{1/2}$. On the other hand, in amperometric experiments with chromaffin cells in hypotonic media, Schroeder et al. observed an increased rate of release (akin to a decreased $t_{1/2}$) for individual events (*24*). In fact, it is postulated that the mechanical pressure that arises from the unfolding of the dense core in chromaffin and chromaffin-like cells provides a significant driving force for the completion of exocytosis, envisioned as the full incorporation of the flattened granular membrane into the plasma membrane (*29*). If this is indeed the case, our data suggest a significant difference in one of the physical driving forces for exocytosis between these cell types and platelets.

While the rate of chemical messenger delivery is not influenced by osmotic pressure, analysis of prespike foot occurrence indicates that the gradient in osmotic pressure between the intragranular and extracellular environment can influence the platelet's ability to subtly modulate chemical messenger release through a fusion pore (*28, 30*). In fact, the percentage of fusion pore events per platelet decreases significantly from 8.1 ± 1.2% under isotonic and 9.7 ± 1.8% under hypertonic conditions to 2.9 ± 1.0% under hypotonic conditions ($p < 0.001$) which is seen in Figure 2B. This trend suggests that the total cytoplasmic and granular membrane tension caused by hypotonic treatment may predominantly contribute to the rapid destabilization of the semistable fusion pore after exocytosis is initiated. Previous reports have described the delicate balance between granular core swelling and dissolution, membrane viscosity, membrane tension, and pore line tension as determinants for the fate of a fusion pore (*29, 31, 32*). The dominating factor may be cell-type-dependent. In the work of Sombers and co-workers, they demonstrated that the foot occurrence changes significantly for vesicles from pharmacologically manipulated and control PC-12 cells and compared foot frequencies to those of other cell types such as mast cells (*33*). It is notable that the foot occurrence of rabbit platelets, 8.1 ± 1.2%, is considerably lower than that, 34 ± 3%, of PC12 cells (*33*) when both cell types are under isotonic conditions, although they share similar vesicle size, approximately 100 nm in radius. As already mentioned, this amperometrically observed difference in foot occurrence may again signify the cell-type-dependent interplay of driving forces in the process of exocytosis. In the case of hypotonic treatment of rabbit platelets, the lowered extracellular osmolarity increased both cytoplasmic and granular membrane tension, with the latter indirectly supported by the data in Figure 2A where granular swelling leads to higher membrane tension (see Broader Distribution of the $Q^{1/3}$ in the Supporting Information). The increased total transpore tension results in an elevated probability of shorter pore lifetime. Subsequently, the foot occurrence for

a group of platelets decreases under hypotonic conditions. However, the decreased transpore tension under hypertonic conditions did not contribute as much as that under hypotonic conditions, suggesting critical roles of other driving forces.

In conclusion, this work presents the first quantitative, real-time measurements of secretion of serotonin from individual granules of isolated platelets. This novel implementation of carbon-fiber microelectrode amperometry yields unprecedented insight into normal platelet function and will facilitate future exploration of abnormal platelet populations and behavior, whether pharmacologically or genetically induced.

ACKNOWLEDGMENT

We gratefully thank Professor James G. White (Department of Laboratory Medicine and Pathology and Pediatrics, University of Minnesota) for helpful discussions and veterinarians Angela M. Craig and Diana M. Freeman (Research Animal Resources, University of Minnesota) for rabbit blood draws.

SUPPORTING INFORMATION AVAILABLE

Experimental details for platelet preparation, preparation of carbon-fiber microelectrodes, electrochemical methods, data acquisition, and statistical analysis. This material is available free of charge via the Internet at http://pubs.acs.org.

REFERENCES

1. Rand, M., and Reid, G. (1951) *Nature 168*, 385.
2. Da Prada, M., Cesura, A. M., Launay, J. M., and Richards, J. G. (1988) *Cell. Mol. Life Sci. 44*, 115–126.
3. Sheridan, D., Carter, C., and Kelton, J. G. (1986) *Blood 67*, 27–30.
4. Kema, I. P., de Vries, E. G. E., and Muskiet, F. A. J. (2000) *J. Chromatogr., B: Biomed. Sci. Appl. 747*, 33–48.
5. Troyer, K. P., Heien, M. L., Venton, B. J., and Wightman, R. M. (2002) *Curr. Opin. Chem. Biol. 6*, 696–703.
6. Travis, E. R., Wang, Y. M., Michael, D. J., Caron, M. G., and Wightman, R. M. (2000) *Proc. Natl. Acad. Sci. U.S.A. 97*, 162–167.
7. Pihel, K., Hsieh, S., Jorgenson, J. W., and Wightman, R. M. (1995) *Anal. Chem. 67*, 4514–4521.
8. Pihel, K., Hsieh, S., Jorgenson, J. W., and Wightman, R. M. (1998) *Biochemistry 37*, 1046–1052.
9. Huizing, M., Anikster, Y., and Gahl, W. A. (2000) *Traffic 1*, 823–835.
10. Neal Pinckard, R., Farr, R. S., and Hanahan, D. J. (1979) *J. Immunol. 123*, 1847–1857.
11. Hochstetler, S. E., Puopolo, M., Gustincich, S., Raviola, E., and Wightman, R. M. (2000) *Anal. Chem. 72*, 489–496.
12. Meyers, K. M., Holmsen, H., and Seachord, C. L. (1982) *Am. J. Physiol. 243*, 454–461.
13. Swamy, B. E., and Venton, B. J. (2007) *Anal. Chem. 79*, 744–750.
14. Fortin, E., Chane-Tune, J., Mailley, P., Szunerits, S., Marcus, B., Petit, J. P., Mermoux, M., and Vieil, E. (2004) *Bioelectrochemistry 63*, 303–306.
15. Kozminski, K. D., Gutman, D. A., Davila, V., Sulzer, D., and Ewing, A. G. (1998) *Anal. Chem. 70*, 3123–3130.
16. Da Prada, M., Pletscher, A., Tranzer, J. P., and Knuchel, H. (1967) *Nature 216*, 1315–1317.
17. Jackson, B. P., Dietz, S. M., and Wightman, R. M. (1995) *Anal. Chem. 67*, 1115–1120.
18. Gerrard, J. M., Rao, G. H. R., and White, J. G. (1977) *Am. J. Pathol. 87*, 633–642.
19. Lam, K. S., Aman, M. G., and Arnold, L. E. (2006) *Res. Dev. Disability 27*, 254–289.
20. Gong, L. W., de Toledo, G. A., and Lindau, M. (2007) *Nat. Cell Biol. 9*, 915–922.
21. Chow, R. H., von Ruden, L., and Neher, E. (1992) *Nature 356*, 60–63.
22. Pollard, H. B., Tack-Goldman, K., Pazoles, C. J., Creutz, C. E., and Shulman, N. R. (1977) *Proc. Natl. Acad. Sci. U.S.A. 74*, 5295–5299.
23. Jacob, S., and Spinler, S. A. (2006) *Ann. Pharmacother. 40*, 1618–1622.
24. Schroeder, T. J., Borges, R., Finnegan, J. M., Pihel, K., Amatore, C., and Wightman, R. M. (1996) *Biophys. J. 70*, 1061–1068.
25. Wightman, R. M., Jankowski, J. A., Kennedy, R. T., Kawagoe, K. T., Schroeder, T. J., Leszczyszyn, D. J., Near, J. A., Diliberto, E. J., Jr., and and Viveros, O. H. (1991) *Proc. Natl. Acad. Sci. U.S.A. 88*, 10754–10758.
26. Borges, R., Travis, E. R., Hochstetler, S. E., and Wightman, R. M. (1997) *J. Biol. Chem. 272*, 8325–8331.
27. Troyer, K. P., and Wightman, R. M. (2002) *J. Biol. Chem. 277*, 29101–29107.
28. Sombers, L. A., Wittenberg, N. J., Maxson, M. M., Adams, K. L., and Ewing, A. G. (2007) *ChemPhysChem 8*, 2471–2477.
29. Amatore, C., Bouret, Y., Travis, E. R., and Wightman, R. M. (2000) *Biochimie 82*, 481–496.
30. Albillos, A., Dernick, G., Horstmann, H., Almers, W., Alvarez de Toledo, G., and Lindau, M. (1997) *Nature 389*, 509–512.
31. Chizmadzhev, Y. A., Kumenko, D. A., Kuzmin, P. I., Chernomordik, L. V., Zimmerberg, J., and Cohen, F. S. (1999) *Biophys. J. 76*, 2951–2965.
32. Chizmadzhev, Y. A., Kuzmin, P. I., Kumenko, D. A., Zimmerberg, J., and Cohen, F. S. (2000) *Biophys. J. 78*, 2241–2256.
33. Sombers, L. A., Hanchar, H. J., Colliver, T. L., Wittenberg, N., Cans, A., Arbault, S., Amatore, C., and Ewing, A. G. (2004) *J. Neurosci. 24*, 303–309.

BI800792M